



# Human Adipose-derived mesenchymal stem cells promote lymphocyte apoptosis and alleviate atherosclerosis via miR-125b-1-3p/BCL11B signal axis

Chaowen Yu, Wenbo Tang, Ran Lu, Yuan Tao, Tiancai Ren, Yong Gao

Department of Vascular Surgery, the First Affiliated Hospital of Bengbu Medical College, Bengbu, China

**Contributions:** (I) Conception and design: Y Gao, W Tang, C Yu; (II) Administrative support: Y Gao, Yuan Tao, C Yu, T Ren; (III) Provision of study materials or patients: T Ren, W Tang, Y Tao; (IV) Collection and assembly of data: C Yu, Y Tao; (V) Data analysis and interpretation: Y Tao, R Lu, T Ren; (VI) Manuscript writing: All authors; (VII) Final approval of manuscript: All authors.

**Correspondence to:** Yong Gao. Department of Vascular Surgery, the First Affiliated Hospital of Bengbu Medical College, Bengbu 233000, China. Email: YongGao0887@hotmail.com.

**Background:** Mesenchymal stem cells (MSCs) have shown great potential in the treatment of cardiovascular diseases, with fat being a more accessible source of MSCs. This study investigated the effect of human adipose-derived mesenchymal stem cells (hMSCs-Ad) exosomes on T lymphocytes and its role in atherosclerosis (AS).

**Methods:** The exosomes were preliminarily isolated hMSCs-Ad and co-cultured with human H9 T lymphocytes. The effects of hMSCs-Ad exosomes on the proliferation and apoptosis of H9 were examined by performing functional experiments. The serum lipid level and inflammatory factor level in tail vein of mice were measured by biochemical analyzer and enzyme linked immunosorbent assay (ELISA) respectively.

**Results:** The hMSCs-Ad-derived exosomes up-regulate the expression of micro (mi)R-125b-1-3p in H9 and AS arterial tissues. miR-125b-1-3p shared a targeted binding site with B-cell chronic lymphocytic leukemia (CLL)/lymphoma 11B gene (BCL11B). miR-125b-1-3p negatively regulated the expression of BCL11B in H9, and that knocking down BCL11B in H9 promoted its apoptosis. Injection of hMSCs-Ad-derived exosomes via the tail vein effectively reduced blood lipid and inflammatory factors, and that relieved the symptoms of AS in AS model mice.

**Conclusions:** miR-125b-1-3p was expressed in hMSCs-Ad exosomes and can promote T lymphocyte apoptosis and alleviate AS by down-regulating BCL11B expression. It provides potential molecular targets for the clinical treatment of AS.

**Keywords:** Adipogenic mesenchymal stem cells; exosomes; miR-125-b-1-3p; atherosclerosis (AS)

Submitted Dec 11, 2020. Accepted for publication Feb 03, 2021.

doi: 10.21037/apm-21-49

View this article at: <http://dx.doi.org/10.21037/apm-21-49>

## Introduction

Mesenchymal stem cells (MSCs), which are multifunctional mesenchymal stromal cells with self-renewal ability, can be found and extracted from almost any mature organ and tissue. According to their intended use, MSCs are generally isolated from umbilical cord blood, fat, dense bone, and other tissues (1). Previous studies have shown that injection of MSCs has a significant effect on protecting

cardiac function (2). The MSCs can produce a large amount of cytokines with immunomodulatory and nutritional properties. Cytokines secreted by MSCs can induce the secretion of relevant cytokines from neighboring cells to exert immunomodulatory effects, and have shown great potential in promoting cardiovascular repair (3). In an ischemic animal model bone marrow, MSCs exert anti-apoptotic and anti-inflammatory effects on cardiac cells

and vascular endothelial cells via paracrine signals (4). The therapeutic effect of MSCs on cardiovascular diseases seems to be mainly due to its paracrine cytokines. The MSCs not only secrete paracrine factors, but also secrete membrane vesicles such as exosomes and microvesicles. Exosomes have a membrane vesicle structure containing biologically active elements such as proteins, miRNAs, and messenger (m)RNAs, and can stably and specifically deliver these molecules to the recipient cells. The MSC exosomes have already been successfully applied in animal models of cardiovascular disease (5,6); thus, administration of MSC exosomes may be a potential method for treating cardiovascular diseases.

The miRNAs, which are a class of small non-coding RNAs with about 22 nucleotides in length, promote the inhibition and degradation of gene translation, and participate in the regulation of cell development and physiological processes by guiding Argonaute proteins into the targeted binding region of mRNA (7). The miRNAs in the circulatory system and exosomes are also considered biomarkers indicative of cardiovascular disease, diabetes, and cancer, and can therefore help in the diagnosis and treatment of diseases (8). The differential expression of miRNA in patients with atherosclerosis (AS) has been confirmed, and miRNAs may be a potential therapeutic target for the reduction of cardiovascular disease (9,10). Of the miRNAs that play an important role in disease occurrence and immune regulation, MiR-125b-1-3p was among the earliest discovered (11). The disease AS involves chronic inflammation of the arterial wall. The main pathogenic factors leading to the occurrence of AS are immune and inflammatory responses and T lymphocyte homeostasis disorder (12). We speculated that miR-125b-1-3p may also participate in the occurrence and development of AS by acting on T lymphocytes and regulating the expression of inflammatory factors.

The MSCs can be extracted from the stromal part of adipose tissues. Due to the easy extraction of fat, adipose tissues contain more abundant stem cell sources than bone marrow and/or other tissues (13), and the process is more easily clinically performed. This study conducted a series of functional experiments predominantly to explore the effect of human adipose-derived mesenchymal stem cell (hMSCs-Ad) exosomes on T lymphocytes, and its possible mechanism of action. In addition, an AS mouse model was established to verify the therapeutic effects of hMSCs-Ad exosomes. We present the following article in accordance with the ARRIVE reporting checklist (available at [http://](http://dx.doi.org/10.21037/apm-21-49)

[dx.doi.org/10.21037/apm-21-49](http://dx.doi.org/10.21037/apm-21-49)).

## Methods

### *Cell culture*

The hMSCs-Ad (Sciencell, Carlsbad, CA, USA) were cultured in mesenchymal stem cell medium (MSCM) (7501, Sciencell) in a 37 °C incubator with 10% CO<sub>2</sub>. Human T lymphocyte H9 were obtained from American Type Culture Collection and was cultured in Roswell Park Memorial Institute (RPMI)-1640 (11879020, Gibco, Fremont, CA, USA) containing 10% fetal bovine serum (FBS) (SV30087.03, GE Hyclone, South Logan, UT, USA) and 1% penicillin-streptomycin (PB180120). After 72 hours, the cells at logarithmic growth stage were taken for subsequent experiments.

### *Extraction and identification of exosomes*

Serum in the medium for culturing hMSCs-Ad at logarithmic phase was replaced with exosome-free serum (A2720803, Gibco, Gaithersburg, MD, USA) to continue the culture. Next, the cells were filtered through a 0.22 μm filter, and concentrated through an ultrafiltration tube. Following the kit instructions (the CSB-EI0102, CUSABIO, Wuhan, Hubei, China), the cells were combined with the corresponding proportion of reagents, thoroughly mixed, and incubated at 4 °C overnight. After centrifuging the cells at 10,000 ×g for 1 hour, the supernatant was then aspirated, and the remaining precipitate was exosomes.

The purified exosomes (10 μL) were diluted with an equal volume of phosphate buffered saline (PBS), transferred to a piece of 2 mm copper mesh, and stood for 1 minute at room temperature. The remaining liquid was gently removed by filter paper and air-dried at room temperature for 2 minutes. The exosomes were observed and photographed under a transmission electron microscope.

### *Cell transfection*

In GeneBank, B-cell chronic lymphocytic leukemia (CLL)/lymphoma 11B gene (BCL11B) small interfering RNA (siRNA) was designed according to NM\_001282237. The sequence of si-BCL11B was 5'-GCCGCCAGCCAAGAGCAAG-3' and the Si-control sequence was 5'-GCCACCGACGAGACGCAAG-3'. The mi-BCL11B and Si-control were transfected into H9

**Table 1** The primer sequences for genes

Genes	Sequences
<i>miR-125b-1-3p</i>	
Forward	5'-ACGGGTTAGGCTCTGGGAGCT-3'
Reverse	5'-CAGTGCGTGTCTGGAGT-3'
<i>U6</i>	
Forward	5'-CTCGCTTCGGCAGCACATATACT-3'
Reverse	5'-ACGCTTCACGAATTTGCGTGTC-3'
<i>BCL11B</i>	
Forward	5'-CGGGCGATGCCAGAATAGAT-3'
Reverse	5'-GATCACGGATGAGTGAGGGT-3'
<i>GAPDH</i>	
Forward	5'-AATGGGCAGCCGTTAGGAAA-3'
Reverse	5'-GATCACGGATGAGTGAGGGT-3'

GAPDH, glyceraldehyde 3-phosphate dehydrogenase.

using Lipofectamine 3000 (L3000015). The transfection efficiency was identified by quantitative polymerase chain reaction (qPCR) 24 hours after the reaction. The study was conducted in accordance with the Declaration of Helsinki (as revised in 2013).

### qPCR

The total RNA in tissues, cells, and exosomes were extracted using the miRNA kit (R8107, GBCBIO Tech., Guangzhou, Guangdong, China) and TRIzol method (15596-026), respectively. The purity and concentration of RNA (OD<sub>260/280</sub> between 1.8–2.0) were detected by an ultraviolet spectrophotometer. The reverse transcription kit (Thermo Fisher, Waltham, MA, USA, K1622) was used for reverse transcription and cDNA library construction. The target gene was amplified by PCR (7500, ABI, Applied Biosystems, Foster City, CA, USA) using reaction solution consisting of 2  $\mu$ L cDNA, 2  $\mu$ L upstream and downstream primers, 10  $\mu$ L BeyoFast™ SYBR Green qPCR Mix (2X) (D7260, Beyotime, Beijing, China), and 6  $\mu$ L Rnase-free water. The PCR conditions were as follows: pre-denaturation at 95 °C for 30 seconds, denaturation at 95 °C for 15 seconds, and annealing extension at 55 °C, for a total of 40 cycles. The  $2^{-\Delta\Delta C_t}$  was used to calculate the relative expressions of target genes. The primer sequences are shown in *Table 1*.

### Detection of H9 cell uptake of PKH67-labeled exosomes

The hMSCs-Ad-derived exosomes were labeled using the PKH67 Green Fluorescent Cell Linker Midi Kit (MIDI67, Sigma-Aldrich, St. Louis, MO, USA). The proliferation of H9 was induced by phytohemagglutinin (L0881, GBCBIO), and the inactivation of hMSCs-Ad was induced by mitomycin C (M1108). A concentration of  $5 \times 10^5$  hMSCs-Ad were inoculated into the upper chamber of Transwell (725101, Nest, Wuxi, Jiangsu, China), while  $1 \times 10^5$  H9 cells were inoculated in the lower chamber. The cells in the two chambers were separated by a semi-permeable membrane but shared the same medium. Exosomes of different concentrations (0, 4, 8, 16  $\mu$ g/ $10^6$ ) were added into the medium for co-culture for 48 hours (14,15). Finally, cells were washed with PBS, fixed with 4% paraformaldehyde for 15 minutes at room temperature, stained with 4',6-diamidino-2-phenylindole (DAPI), washed with PBS, and the cellular uptake of PKH 67-labeled exosomes was observed by confocal microscopy.

### Cell proliferation

The H9 cells were inoculated to a 96-well plate, and combined with 10 L cell counting kit-8 (CCK-8, YZ-CK04, Solarbio, Beijing, China) and 100 L RPMI-1640 to culture for 48 hours. After 3 hours culture, the optical density (OD) value of each well at the wavelength of 450 nm was detected by a marker enzyme (FC, Thermo Fisher). The cell survival rate was calculated as: experiment well OD-blank hole OD/control well OD-blank hole OD  $\times 100\%$ .

### Dual-luciferase reporter gene

The target genes for miR-125b-1-3p were predicted by TargetScan ([www.targetscan.org/vert\\_72/](http://www.targetscan.org/vert_72/)) and further confirmed by dual-luciferase reporter. Luciferase reporter plasmids of BCL11B mutant (BCL11B-MUT) and BCL2L11 wild-type (BCL11B-WT) were constructed and co-transfected with miR-125b-1-3p mimics and negative control (NC) using Lipofectamine 3000. The fluorescence intensity was measured 48 hours later using a dual-luciferase reporter kit (RG009, Beyotime).

### Annexin V-FITC/PI

The H9 cells were rinsed in PBS, mixed with 1 mL 70% cold ethanol, fixed at 4 °C for 2 hours, centrifuged at 1,000  $\times$ g

for 4 minutes, and precipitated. Annexin V-fluorescein isothiocyanate (FITC) and propidium iodide (PI) staining solution (630110, Clontech, Mountain View, CA, USA) were added, mixed with the cells, and incubated at room temperature in the dark for 15 minutes. Finally, cell apoptosis was detected by flow cytometry (322457, Bio-Rad, Hercules, CA, USA).

### *Cell cycle detection*

The cell operation was conducted as above. A total of 0.5 mL PI staining solution was added to the cells to react at 4 °C in the dark for 30 minutes. The red fluorescence at 488 nm was detected by flow cytometry, and the cell cycle distribution of each group was analyzed by BD software (Becton, Dickinson and Co., Franklin Lakes, NJ, USA).

### *Western blot*

Radioimmunoprecipitation assay (RIPA, G3424, Gbcbio) was used to lyse cells for obtaining protein samples. The proteins were separated on 12% sodium dodecyl sulfate-polyacrylamide gel electrophoresis (SDS-PAGE) gel and then transferred to polyvinylidene difluoride (PVDF) membrane by wet method. Then, BCL11B (MA5-31434, Thermo-Fisher), BCL-2 (MA5-11757), Bax (MA5-14003), and glyceraldehyde 3-phosphate dehydrogenase (GAPDH, 437000) were added to incubate with the proteins at room temperature for 2 hours. The membrane was combined with the primary antibody and incubated overnight at 4 °C, then rinsed 3 times in PBS, combined with the secondary antibody (A32723) for incubation at room temperature for 30 minutes, and then washed 3 times. Chemiluminescence was used for color development and fixation. Each strip was analyzed and scanned by the gel image processing system.

### *Construction of AS mouse model*

A total of 20 6-week-old C57BL/6 background ApoE<sup>-/-</sup> mice were purchased from Jackson Laboratory (Bar Harbor, ME, USA), and were evenly divided into an AS model group and exosome group, with normal C57BL/6 mice as the control group (CON group, n=10). There was no difference in gender, age, or feeding environment among all the mice. The CON group was fed a normal diet containing 5% fat, while the rest were fed a high-fat diet containing 0.2% cholesterol and 20% fat. After 2 weeks of

feeding, mice with a high-fat diet were intraperitoneally injected with 10% chloral hydrate (5 mL/kg) to be anesthetized, and their right common carotid artery was isolated, exposed, and placed with a perivascular collar. The artery was then closed, and the operated mice were fed for a further 8 weeks (16).

### *Blood lipid test*

Venous blood was collected from the bilateral inner canthus veins of mice, and the levels of total cholesterol (TC), triglyceride (TG), high-density lipoprotein cholesterol (HDL-C), and low-density lipoprotein cholesterol (LDL-C) were detected by a biochemical analyzer (Hitachi 7600, Chiyoda, Tokyo, Japan).

### *Enzyme-linked immunosorbent assay*

Mouse serum was collected and centrifuged at 1,000 rpm for 10 minutes, and the expressions of interferon-gamma (IFN- $\gamma$ ), tumor necrosis factor-alpha (TNF- $\alpha$ ) (CSB-E04741m, CUSABIO), interleukin-6 (IL-6, CSB-E04639m, CUSABIO), and angiotensin-II (Ang-II, JL11512, Jianglai Bio., Shanghai, China) were detected according to the kit instructions (EK0375, Sciencell). The sample was added to the plate, sealed, and incubated for 30 minutes at 37 °C. The liquid was discarded and the cells were washed 5 times. Apart from the blank wells, 50  $\mu$ L of enzyme labeling reagent was added to each well and incubated at 37 °C for 30 minutes. After washing, 50  $\mu$ L A and B color reagents were added to the plate at 37 °C in the dark for 15 minutes. Finally, the reaction was terminated by adding 50  $\mu$ L stop solution. The blank well was adjusted to 0, and the OD value of each well was read at 450 nm using a microplate reader within 15 minutes following the reaction. The concentration of the target factor was calculated according to the standard curve.

All animal experiments were performed in accordance with the guidelines for animal care and approved by the regional ethics committee of Bengbu Medical College (No.: 20190213).

### *Statistical analysis*

The data were shown as mean  $\pm$  SD. Independent sample *t*-test, Pearson test, one-way analysis of variance (ANOVA), and repeated measurement ANOVA were used for statistical

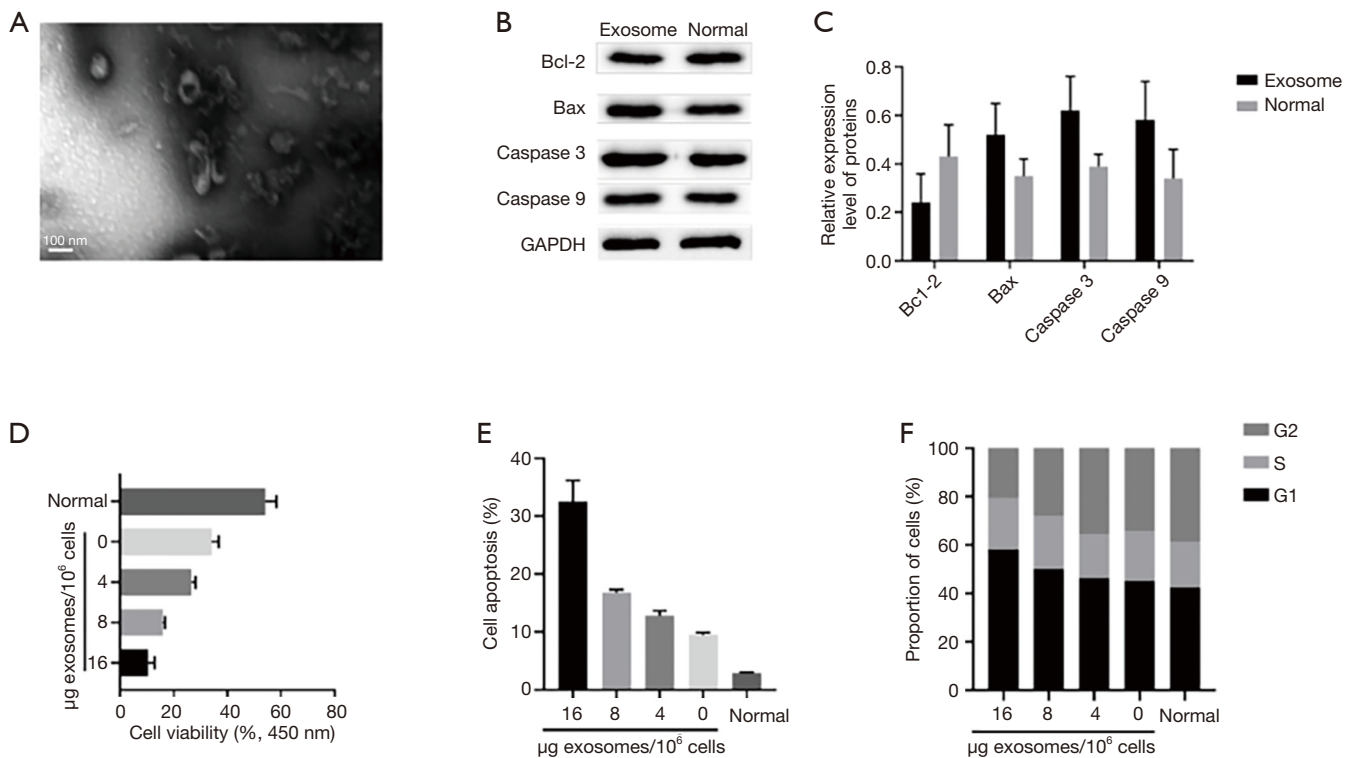


**Figure 1** Co-culture of hMSCs-ad exosomes at different concentrations with H9 cells. (A) Exosome morphology observed under an electron microscope; (B,C) Western blot to detect protein expression; (D) CCK-8 to detect cell activity; (E,F) flow cytometry to detect apoptosis and cell cycle. hMSCs-ad, human adipose-derived mesenchymal stem cells; CCK-8, cell counting kit-8.

analysis in GraphPad prism version 8 (GraphPad software, San Diego, CA, USA). A P value <0.05 was considered statistically significant.

## Results

### *hMSCs-Ad was co-cultured with H9 cells*

Under the electron microscope, we observed that exosomes were saucer-shaped or hemispherical with a concave side, diameter of about 30–100 nm, and a complete membrane structure. The proliferation of H9 cells decreased with the increase of the exosome concentration, and the cell apoptosis increased significantly when the exosome concentration reached 16  $\mu\text{g}/10^6$ ; moreover, the proportion of the cells in G1 phase also increased greatly. Western blot analysis showed that the expression of anti-apoptotic protein Bcl-2 in H9 cells was down-regulated, while the expression of Bax, Caspase 3, and Caspase 9 proteins was up-regulated when the exosome concentration was 16  $\mu\text{g}/10^6$  (Figure 1).

### *The hMSCs-Ad-derived exosomes up-regulate the expression of miR-125b-1-3p in H9 and AS arterial tissues*

We performed qPCR to detect the miR-125b-1-3p expression in hMSCs-Ad and exosomes (16  $\mu\text{g}/10^6$ ), and the results showed that miR-125b-1-3p expression in exosomes was significantly up-regulated. Co-culture of hMSCs-Ad and their exosomes (16  $\mu\text{g}/10^6$ ) with H9 up-regulated the expression of miR-125b-1-3p in H9. The expression of miR-125b-1-3p was low in the arterial tissues of the AS model, but it was up-regulated after the injection of hMSCs-Ad exosomes (16  $\mu\text{g}/10^6$ ) via tail vein into the mice (Figure 2).

### *miR-125b-1-3p targeted and regulated the expression of BCL11B*

TargetScan was used to predict the binding sites between miR-125b-1-3p and BCL11B. Dual-luciferase reporter



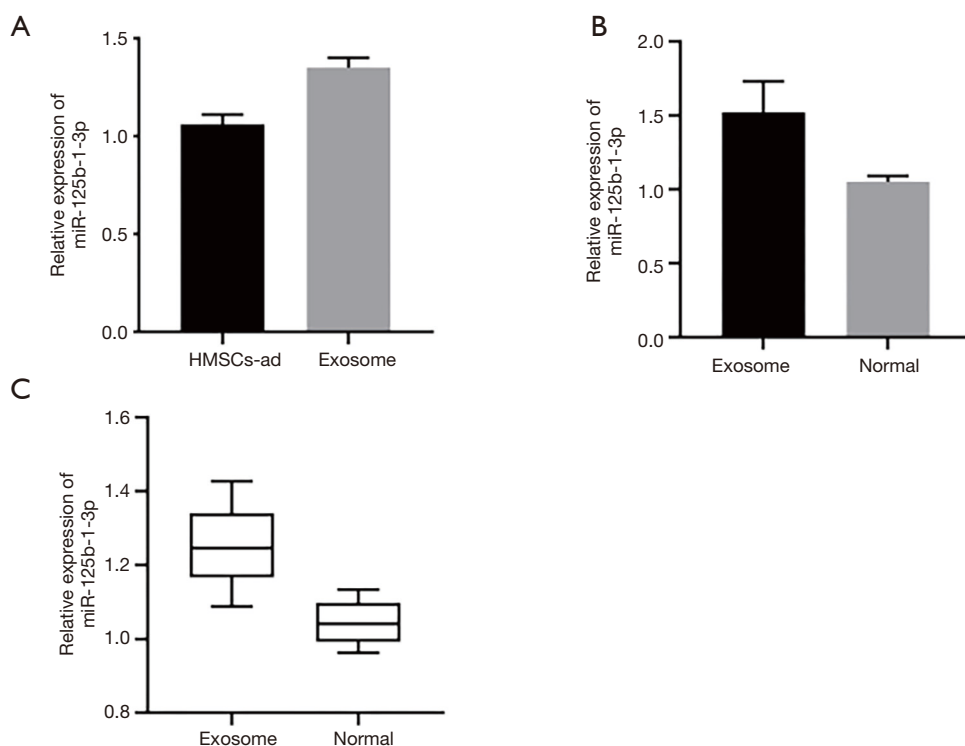


**Figure 2** hMSCs-Ad exosomes can up-regulate the expression of miR-125b-1-3p in H9 cells and AS arterial tissues. (A) qPCR detection of miR-125b-1-3p expression in HMSCs-ads and exosomes; (B) qPCR detection of miR-125b-1-3p expression in H9 cells; (C) qPCR detection of miR-125b-1-3p expression in mouse arterial tissues. hMSCs-Ad, human adipose-derived mesenchymal stem cells; qPCR, quantitative polymerase chain reaction; AS, atherosclerosis.

assay showed that the luciferase activity decreased when BCL11B-WT was co-transfected with miR-125b-1-3p mimics ( $P < 0.05$ ). Detection by qPCR found that the mRNA expression of BCL11B in the AS model group was significantly higher than that in the CON group ( $P < 0.05$ ). Pearson test was used to analyze the correlation between miR-125b-1-3p and BCL11B in the tissues of the AS model group, and the results showed that the relative expression of miR-125b-1-3p was negatively correlated with mRNA expression of BCL11B, and that miR-125b-1-3p negatively regulated the expression of BCL11B (Figure 3).

#### **Knocking out BCL11B promoted apoptosis of lymphocytes**

Transfection efficiency was detected by qPCR and western blot. After the transfection, si-BCL11B was low-expressed in H9 cells. The data of CCK-8, flow cytometry, and western blot revealed that in the si-BCL11B group the proliferation of H9 cells was significantly decreased, apoptosis rate was increased, cell cycle was blocked, and

apoptotic protein expressions were up-regulated (Figure 4).

#### **hMSCs-Ad exosomes relieved the symptoms of AS**

The levels of TC, TG, and LDL-C in the AS model group were significantly higher than those in the CON group ( $P < 0.05$ ). Enzyme-linked immunosorbent assay (ELISA) revealed that serum IFN- $\gamma$ , TNF- $\alpha$ , IL-6, and Ang-II in the mice of the AS group were significantly higher than the CON group ( $P < 0.05$ ). Inflammatory factor levels in serum were significantly reduced in tail intravenous HMSCs-ad extrapyramidal mice ( $P < 0.05$ ) (Figure 5).

#### **Discussion**

The incidence of cardiovascular diseases is increasing rapidly and it has become a major cause of death all over the world (17,18), which necessitates improving the prevention and control of cardiovascular diseases and the disease prognosis. The disease AS, which is the main

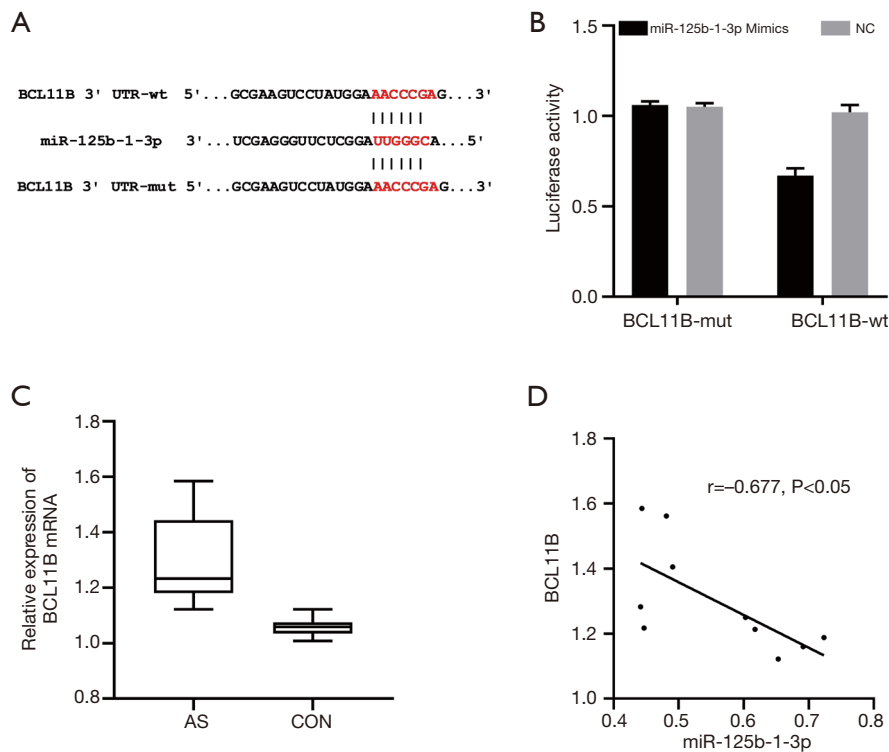


**Figure 3** miR-125b-1-3p can target and regulate BCL11B. (A) The binding site between miR-125b-1-3p and BCL11B; (B) dual-luciferase reporter on genes; (C) qPCR detection of mRNA expression of BCL11B in AS model group tissues; (D) Pearson's test to analyze the correlation between miR-125b-1-3p and BCL11B. qPCR, quantitative polymerase chain reaction.

cause of coronary heart and peripheral vascular disease (19,20), is a result of atherosclerotic plaque formation (21). Inflammation and lipid accumulation play a key role in the occurrence and development of AS. Visceral fat deposition can lead to an increased risk of AS and cardiac metabolism, and excessive visceral fat is closely associated with AS (22). Therefore, in this study, ApoE<sup>-/-</sup> mice were fed a high-fat diet, and a perivascular cuff was placed on the common carotid artery to construct an AS mouse model. Neeland *et al.* (22) showed that high lipid level could be an independent risk factor for predicting the occurrence and death of AS patients, which was consistent with our results that AS mice showed higher lipids than those in the CON group. In addition, Neeland (22) also found a causal relationship between high lipid level and inflammation, which is supported by genetic evidence, and lipoprotein marked by high triglyceride was an important cause of inflammation, AS, and mortality of patients.

The arterial disease AS is an inflammatory disease related to lipid metabolism (23). The active inflammatory process may cause plaque rupture and increase the risk

of developing coronary thrombosis. Innate and adaptive immunity play an important role in AS. Macrophages and T lymphocytes have potent proatherogenic effects, and defects of T lymphocytes can significantly inhibit the development of AS lesions (24,25). In the arterial wall, subendothelial retention of atherogenic lipoproteins can trigger T cells to form AS plaques. Inflammation is caused by the innate immune response of modified lipoproteins, and T lymphocytes remain active in AS lesions (26).

As a stromal vascular residue in adipose tissue, hMSCs-Ad are directly involved in the self-renewal and self-repair of cells in the body, while the inflammatory state in cardiovascular diseases can directly affect the proliferation, differentiation, and regeneration of hMSCs-Ad (27). The MSCs have a dual effect in transforming cells from pro-inflammatory to anti-inflammatory or pro-inflammatory phenotypes (28). Studies (29) have found that MSCs can effectively inhibit T lymphocyte proliferation and T lymphocyte receptor activation, reduce cytokine secretion and cytotoxicity, and regulate the balance of Th1/Th2 and T cell function *in vitro*. Compared with other MSCs,

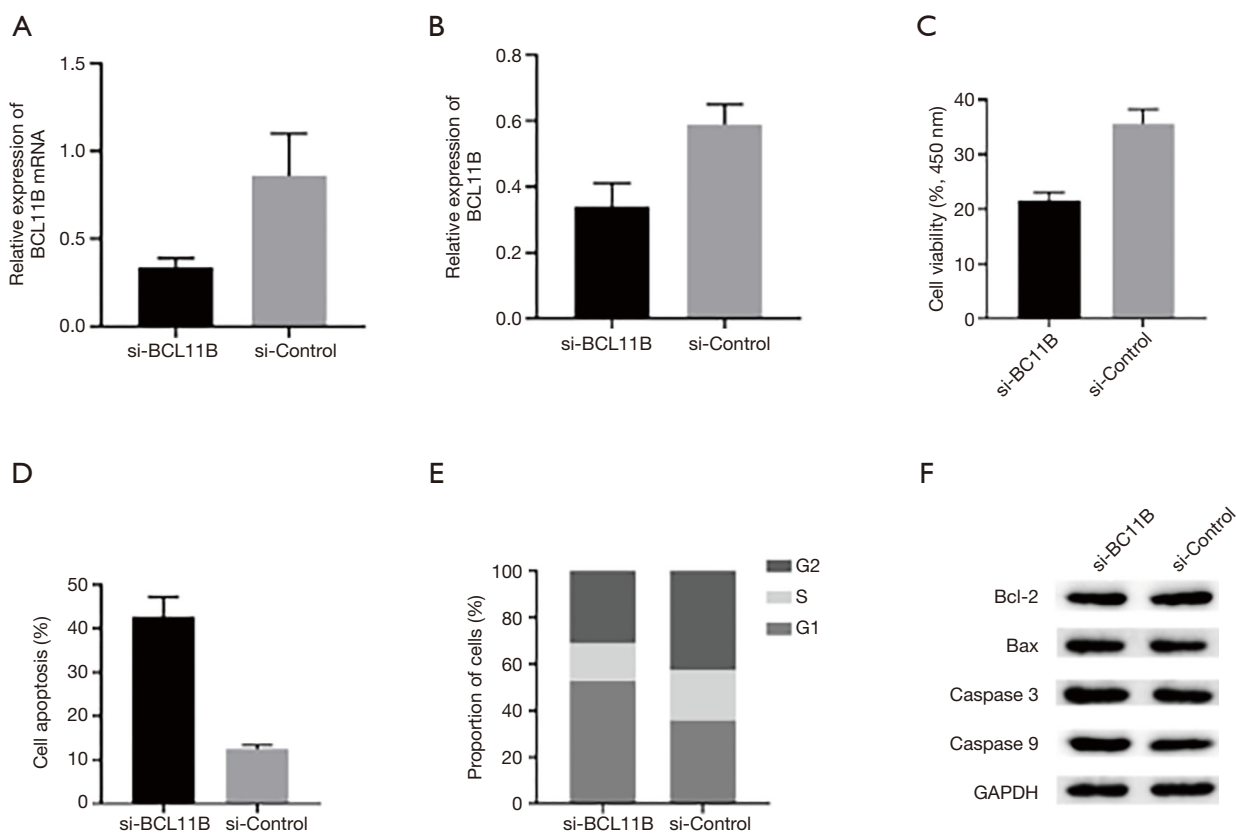


**Figure 4** miR-125b-1-3p can inhibit the expression of BCL11B to promote the proliferation of T lymphocytes. (A,B) qPCR and western blot detection of transfection efficiency of si-BCL11B; (C) CCK-8 detection of cell proliferation; (D,E) flow cytometry to detect apoptosis and cell cycle; (F) Western blot detection of apoptotic protein expressions. qPCR, quantitative polymerase chain reaction; CCK-8, cell counting kit-8.

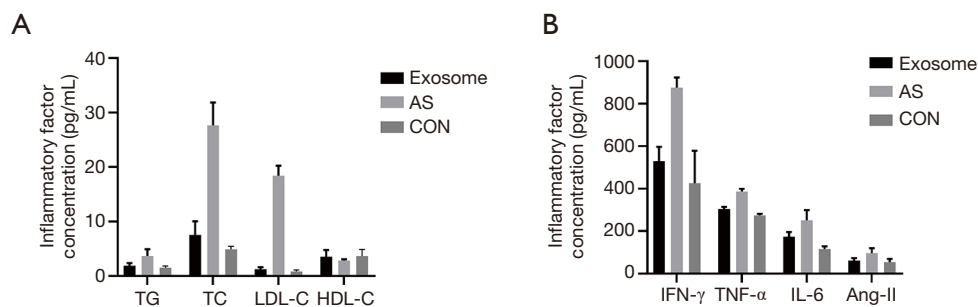


**Figure 5** hMSCs-Ad exosomes reduced AS symptoms. (A) Detection of blood lipids in mice; (B) ELISA detection of expressions of inflammatory factors. hMSCs-Ad, human adipose-derived mesenchymal stem cells; ELISA, enzyme-linked immunosorbent assay; AS, atherosclerosis.

hMSCs-Ad have a stronger immunosuppressive effect on T lymphocyte activation and B lymphocyte function inhibition. The hMSCs-Ad are expected to be a therapeutic

agent with immunosuppressive effect (30). The results of this study indicated that after co-culture of hMSCs-Ad with its exosomes, there was inhibition of the proliferation of H9



cells, increased G1 cell proportion, and significant change in the expressions of apoptosis-related proteins, indicating that hMSCs-Ad and its exosomes could promote T lymphocyte apoptosis.

The hMSCs-Ad can release a large number of exosomes that carry miRNAs to target organs into the peripheral environment, thus enhancing organ function in various chronic diseases and delaying disease progression (31). Zhu *et al.* (32) found that miR-125b-1-3p in exosomes secreted by MSCs under anoxic environment can regulate apoptosis of myocardial cells, thus promoting ischemic heart repair. This suggests that the exosomes secreted by MSCs carry miR-125-1-3p, which mediates apoptosis of cells and plays a targeted role in myocardial repair. In mouse myocardial ischemia-reperfusion model with high-expressed miR-125b, miR-125 protects the myocardium from ischemia/reperfusion (I/R) damage by inhibiting p53-mediated apoptotic signals and NF- $\kappa$ B activation mediated by TRAF 6, thus significantly reducing the myocardial infarction and preventing cardiac insufficiency (33). Li *et al.* (34) transfected miR-125b-1-3p mimics into mouse cardiomyocytes, and the oxidative stress and apoptotic protein expressions were significantly increased. Other studies revealed that umbilical cord-derived MSCs significantly inhibit T lymphocyte proliferation by inducing T lymphocyte apoptosis and cell cycle arrest (14).

In this study, we found that hMSCs-Ad exosomes could secrete miR-125b-1-3p. Moreover, bioinformatics analysis and dual-luciferase reporter gene showed that there was a targeted binding region between miR-125b-1-3p and BCL11B. Pearson test analysis of qPCR results demonstrated that miR-125b-1-3p could inhibit the expression of BCL11B in the AS mice. Knocking out BCL11B expression in H9 cells showed that the pro-apoptotic effect of hMSCs-Ad exosomes was ineffective. The protein BCL11B, which plays an important role in the differentiation, proliferation, and survival of T lymphocyte immune T cells (35), connects directly to a promoter or indirectly via heterologous DNA binding domains to cause transcriptional repression (36). Huang *et al.* (37) demonstrated that in leukemia inhibition of BCL11B can effectively suppress the proliferation of T cells and induce cell apoptosis, suggesting that BCL11B siRNA could be explored as a novel targeted therapy strategy to maintain T cell homeostasis, and this also supports our findings.

An *in vivo* experiment found that intravenous injection of hMSCs-Ad exosomes could effectively reduce the blood lipid level of AS mice, and reduce the levels of inflammatory

factors IFN- $\gamma$ , TNF- $\alpha$ , IL-6, and Ang-II. The current findings demonstrated the role of hMSCs-Ad exosomes in the treatment of AS. We speculated that hMSCs-Ad exosomes could secrete miR-125b-1-3p to target the expression of BCL11B in T lymphocytes (38-40).

In conclusion, hMSCs-Ad could secrete exosomes containing miR-125b-1-3p, and it could target and regulate the expression of BCL11B in T lymphocytes after the absorption of vesicles by T lymphocytes, thus blocking the cell cycle, increasing cell apoptosis, inhibiting cell proliferation, and thereby reducing inflammation and blood lipid in AS mice.

### Acknowledgments

*Funding:* This study was supported by the Key Research and Development Plan Projects of the Anhui Province (201904a07020020).

### Footnote

*Reporting Checklist:* The authors have completed the ARRIVE reporting checklist. Available at <http://dx.doi.org/10.21037/apm-21-49>

*Data Sharing Statement:* Available at <http://dx.doi.org/10.21037/apm-21-49>

*Conflicts of Interest:* All authors have completed the ICMJE uniform disclosure form (available at <http://dx.doi.org/10.21037/apm-21-49>). The authors have no conflicts of interest to declare.

*Ethical Statement:* The authors are accountable for all aspects of the work in ensuring that questions related to the accuracy or integrity of any part of the work are appropriately investigated and resolved. All animal experiments were performed in accordance with the guidelines for animal care and approved by the regional ethics committee of Bengbu Medical College (No.: 20190213). The study was conducted in accordance with the Declaration of Helsinki (as revised in 2013).

*Open Access Statement:* This is an Open Access article distributed in accordance with the Creative Commons Attribution-NonCommercial-NoDerivs 4.0 International License (CC BY-NC-ND 4.0), which permits the non-commercial replication and distribution of the article with

the strict proviso that no changes or edits are made and the original work is properly cited (including links to both the formal publication through the relevant DOI and the license). See: <https://creativecommons.org/licenses/by-nc-nd/4.0/>.

## References

- Volarevic V, Arsenijevic N, Lukic ML, et al. Concise review: mesenchymal stem cell treatment of the complications of diabetes mellitus. *Stem Cells* 2011;29:5-10.
- Faiella W, Atoui R. Therapeutic use of stem cells for cardiovascular disease. *Clin Transl Med* 2016;5:34.
- Ranganath SH, Levy O, Inamdar MS, et al. Harnessing the mesenchymal stem cell secretome for the treatment of cardiovascular disease. *Cell Stem Cell* 2012;10:244-58.
- Tang YL, Zhao Q, Qin X, et al. Paracrine action enhances the effects of autologous mesenchymal stem cell transplantation on vascular regeneration in rat model of myocardial infarction. *Ann Thorac Surg* 2005;80:229-36; discussion 236-7.
- Suzuki E, Fujita D, Takahashi M, et al. Stem cell-derived exosomes as a therapeutic tool for cardiovascular disease. *World J Stem Cells* 2016;8:297-305.
- Suzuki E, Fujita D, Takahashi M, et al. Therapeutic Effects of Mesenchymal Stem Cell-Derived Exosomes in Cardiovascular Disease. *Adv Exp Med Biol* 2017;998:179.
- Gebert LFR, MacRae IJ. Regulation of microRNA function in animals. *Nat Rev Mol Cell Biol* 2019 20:21-37.
- Wang J, Chen J, Sen S. MicroRNA as biomarkers and diagnostics. *J Cell Physiol* 2016;231:25-30.
- Jones Buie JN, Goodwin AJ, Cook JA, et al. The role of miRNAs in cardiovascular disease risk factors. *Atherosclerosis* 2016;254:271-81.
- Feinberg MW, Moore KJ. MicroRNA regulation of atherosclerosis. *Circ Res* 2016;118:703-20.
- Li Q, Pan Z, Wang X, et al. miR-125b-1-3p inhibits trophoblast cell invasion by targeting sphingosine-1-phosphate receptor 1 in preeclampsia. *Biochem Biophys Res Commun* 2014;453:57-63.
- Profumo E, Buttari B, Petrone L, et al. Redox imbalance of red blood cells impacts T lymphocyte homeostasis: implication in carotid atherosclerosis. *Thromb Haemost* 2011;106:1117-26.
- Casteilla L, Planat-Benard V, Laharrague P, et al. Adipose-derived stromal cells: their identity and uses in clinical trials, an update. *World J Stem Cells* 2011;3:25.
- Li X, Xu Z, Bai J, et al. Umbilical Cord Tissue-Derived Mesenchymal Stem Cells Induce T Lymphocyte Apoptosis and Cell Cycle Arrest by Expression of Indoleamine 2, 3-Dioxygenase. *Stem Cells Int* 2016;2016:7495135.
- Blazquez R, Sanchez-Margallo FM, de la Rosa O, et al. Immunomodulatory potential of human adipose mesenchymal stem cells derived exosomes on in vitro stimulated T cells. *Front Immunol* 2014;5:556.
- Liu Y, Cheng P, Wu A. Honokiol inhibits carotid artery atherosclerotic plaque formation by suppressing inflammation and oxidative stress. *Aging (Albany NY)* 2020;12:8016-28.
- Joseph P, Leong D, McKee M, et al. Reducing the global burden of cardiovascular disease, part 1: the epidemiology and risk factors. *Circ Res* 2017;121:677-94.
- Leong DP, Joseph PG, McKee M, et al. Reducing the global burden of cardiovascular disease, part 2: prevention and treatment of cardiovascular disease. *Circ Res* 2017;121:695-710.
- Katsiki N, Mantzoros C, Mikhailidis DP. Adiponectin, lipids and atherosclerosis. *Curr Opin Lipidol* 2017;28:347-54.
- Shu J, Santulli G. Update on peripheral artery disease: epidemiology and evidence-based facts. *Atherosclerosis* 2018;275:379-81.
- Zapolski T, Furmaga J, Jaroszyński A, et al. The reverse remodeling of the aorta in patients after renal transplantation - the value of aortic stiffness index: prospective echocardiographic study. *BMC Nephrol* 2017;18:33.
- Neeland IJ, Ross R, Després JP, et al. Visceral and ectopic fat, atherosclerosis, and cardiometabolic disease: a position statement. *Lancet Diabetes Endocrinol* 2019;7:715-25.
- Zhang C, Wang K, Yang L, et al. Lipid metabolism in inflammation-related diseases. *Analyst* 2018;143:4526-36.
- Taleb S. Inflammation in atherosclerosis. *Arch Cardiovasc Dis* 2016;109:708-15.
- Cheng F, Twardowski L, Reifenberg K, et al. Combined B, T and NK cell deficiency accelerates atherosclerosis in BALB/c mice. *PLoS One* 2016;11:e0157311.
- Gisterå A, Hansson GK. The immunology of atherosclerosis. *Nat Rev Nephrol* 2017;13:368.
- Badimon L, Cubedo J. Adipose tissue depots and inflammation: effects on plasticity and resident mesenchymal stem cell function. *Cardiovasc Res* 2017;113:1064-73.
- Zimmermann JA, Hettiaratchi MH, McDevitt TC. Enhanced immunosuppression of T cells by sustained presentation of bioactive interferon- $\gamma$  within three-

- dimensional mesenchymal stem cell constructs. *Stem Cells Transl Med* 2017;6:223-37.
29. Gao F, Chiu SM, Motan DAL, et al. Mesenchymal stem cells and immunomodulation: current status and future prospects. *Cell Death Dis* 2016;7:e2062.
  30. Ribeiro A, Laranjeira P, Mendes S, et al. Mesenchymal stem cells from umbilical cord matrix, adipose tissue and bone marrow exhibit different capability to suppress peripheral blood B, natural killer and T cells. *Stem Cell Res Ther* 2013;4:125.
  31. Baranova A, Maltseva D, Tonevitsky A. Adipose may actively delay progression of NAFLD by releasing tumor-suppressing, anti-fibrotic miR-122 into circulation. *Obes Rev* 2019;20:108-18.
  32. Zhu LP, Tian T, Wang JY, et al. Hypoxia-elicited mesenchymal stem cell-derived exosomes facilitates cardiac repair through miR-125b-mediated prevention of cell death in myocardial infarction. *Theranostics* 2018;8:6163-77.
  33. Wang X, Ha T, Zou J, et al. MicroRNA-125b protects against myocardial ischaemia/reperfusion injury via targeting p53-mediated apoptotic signalling and TRAF6. *Cardiovasc Res* 2014;102:385-95.
  34. Li Q, Qin M, Li T, et al. Rutin protects against pirarubicin-induced cardiotoxicity by adjusting microRNA-125b-1-3p-mediated JunD signaling pathway. *Mol Cell Biochem* 2020;466:139-48.
  35. Longabaugh WJR, Zeng W, Zhang JA, et al. Bcl11b and combinatorial resolution of cell fate in the T-cell gene regulatory network. *Proc Natl Acad Sci U S A* 2017;114:5800-7.
  36. Cismasiu VB, Adamo K, Gecewicz J, et al. BCL11B functionally associates with the NuRD complex in T lymphocytes to repress targeted promoter. *Oncogene* 2005;24:6753-64.
  37. Huang X, Chen S, Shen Q, et al. Down regulation of BCL11B expression inhibits proliferation and induces apoptosis in malignant T cells by BCL11B-935-siRNA. *Hematology* 2011;16:236-42.
  38. Xie Q, Gu X, Chen J, et al. Soyasaponins Reduce Inflammation and Improve Serum Lipid Profiles and Glucose Homeostasis in High Fat Diet-Induced Obese Mice. *Mol Nutr Food Res* 2018;62:e1800205.
  39. Chen WQ, Zhong L, Zhang L, et al. Oral rapamycin attenuates inflammation and enhances stability of atherosclerotic plaques in rabbits independent of serum lipid levels. *Br J Pharmacol* 2009;156:941-51.
  40. Mu H, Wang L, Zhao L. HSP 90 inhibition suppresses inflammatory response and reduces carotid atherosclerotic plaque formation in ApoE mice. *Cardiovasc Ther* 2017;35:e12243.

(English Language Editor: J. Jones)

**Cite this article as:** Yu C, Tang W, Lu R, Tao Y, Ren T, Gao Y. Human Adipose-derived mesenchymal stem cells promote lymphocyte apoptosis and alleviate atherosclerosis via miR-125b-1-3p/BCL11B signal axis. *Ann Palliat Med* 2021;10(2):2123-2133. doi: 10.21037/apm-21-49